Phononic crystals' band gap manipulation via displacement modes

Valiya Valappil, Sabiju; Aragón, Alejandro M.; Goosen, Hans

DOI
10.1016/j.ssc.2022.115061

Publication date
2023

Document Version
Final published version

Published in
Solid State Communications

Solid State Communications 361 (2023) 115061

Contents lists available at ScienceDirect

Solid State Communications

journal homepage: www.elsevier.com/locate/ssc

Communication

Phononic crystals' band gap manipulation via displacement modes☆

Sabiju Valiya Valappil *, Alejandro M. Aragón, Hans Goosen

Faculty of Mechanical, Maritime and Material Engineering, Delft University of Technology, Mekelweg 2, 2628CD, Delft, The Netherlands

ARTICLE INFO

Communicated by Xu Wen

Keywords:
Phononic crystals
Brillouin zone
Displacement modes
Partial band gaps

ABSTRACT

Phononic crystal band gaps (BGs), which are realized by Bragg scattering, have a central frequency and width related to the unit cell's size and the impedance mismatch between material phases. BG tuning has generally been performed by either trial and error or by computational tools such as topology optimization. In either case, understanding how to systematically change the design for a particular band structure is missing. This paper addresses this by closely studying the displacement modes within the wavebands that are responsible for the BG. We look at the variation in different displacement modes due to the changes in the geometry and correlate these changes to their corresponding band structures. We then use this insight to design the unit cell for a particular application, for instance, for generating partial BGs.

1. Introduction

Phononic crystals (PnCs) are artificial materials that rely on the periodicity of scatterers in a matrix to derive unusual properties, such as band gaps (BGs), which are frequency ranges where mechanical waves are attenuated [1,2]. These BGs are generated because of the destructive interference of waves due to Bragg scattering at material interfaces of the periodic unit cell (PUC) [3]. As a result, PnCs are currently being explored in various applications, such as vibration isolation [4], energy harvesting [5,6], wave steering [7,8], and acoustic cloaking [9,10], among others [11,12].

BGs can be identified by means of the PnCs band structure (or dispersion relation) [13], which is obtained by solving a series of eigenvalue problems that are derived by considering a finite set of wave vectors along the irreducible Brillouin zone (IBZ) [14] and prescribing their corresponding Bloch–Floquet periodic boundary conditions [15]. The achieved band structure relates the frequency to the wave vector and provides us with the wave speeds of different wavebands (frequency bands present in the band structure) and BGs. An example is shown in Fig. 1 with the PUC, its IBZ (marked inside the first Brillouin zone), and the band structure with the BG (shaded region).

For designing PnCs, it is essential to understand how changing the geometric features of the PUC affects the band structure. As BGs in PnCs are generated due to Bragg scattering, the BG central frequency is related to the dimensions of the PUC (Bragg's law of diffraction [3]). As a result, scaling the PUC geometry allows us to shift the BG in the frequency domain. Moreover, the BG width is directly related to the impedance mismatch between the material phases within the PUC. Hence, changing this feature allows tuning of the BG width. Band structure manipulation, in general, is conducted either by trial and error or by using existing designs with specific known BG properties that can be subjected to minor changes—for instance, tuning partial BGs (PBGs) of topological PnCs [16]. PBGs are intriguing features because unlike a complete BG, PBGs possess directional aspects, *i.e.,* using PBGs, we can control the propagation direction of incoming waves. PBGs are used in applications including directional waveguiding [17] and medical imaging [18]. However, to obtain PBGs, one needs to break the spatial symmetry in the structure, thus making the design process more intricate. Hence sophisticated computational tools such as topology optimization [19] have also been used for designing PnCs with PBG. Nevertheless, the relation between different wavebands, variations of wavebands with regard to the PUC geometry, and other factors affecting their changes have not fully been explored.

We proposes a design approach to make informed changes to the PUC geometry to achieve a desired BG based on the displacement modes associated with specific points in the band structure. We apply this approach to design 2D PnCs possessing PBGs from an initial design having a complete BG.

2. Analysis of a 2D solid phononic crystal

Consider a single phase 2D PnC composed of a solid material as shown in Fig. 1(a) where the geometric parameters, a, w, and t, are

☆ This document is the results of the research project funded by the Topconsortia voor Kennis en Innovatie (TKI), The Netherlands project grant.

* Correspondence to: Department of Precision and Microsystems Engineering, Faculty of Mechanical, Maritime and Material Engineering, Delft University of Technology, Mekelweg 2, 2628CD, Delft, The Netherlands.

E-mail addresses: S.ValiyaValappil@tudelft.nl (S. Valiya Valappil), A.M.Aragon@tudelft.nl (A.M. Aragón), J.F.L.Goosen@tudelft.nl (H. Goosen).

https://doi.org/10.1016/j.ssc.2022.115061
Received 19 September 2022; Received in revised form 21 December 2022; Accepted 24 December 2022
Available online 28 December 2022

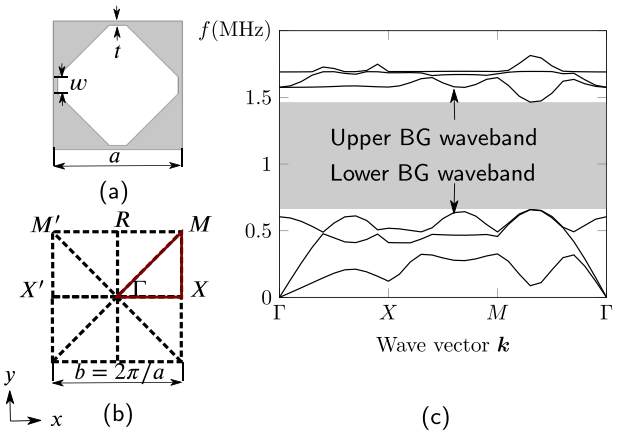

Fig. 1. Schematic of a 2D PnC: (a) the PUC where the lattice length $a = 0.75\,\text{mm}$, width and thickness of the thin sections, $w = 0.1\,\text{mm}$, and $t = 0.025\,\text{mm}$, respectively, are marked, (b) the complete Brillouin zone (dashed lines) with the dimension b and the triangular IBZ (solid lines), (c) corresponding band structure with the shaded region representing the BG bounded by upper and lower wavebands.

marked using arrows. The particular shape of this initial design is irrelevant since the only objective of this design is to possess a BG, which can be achieved by various means. For instance, a two-phase design where a spherical (or any other shaped) scatterer in a substrate structure would also possess a BG and can be used as the initial design. However, a single-phase design is easier to manufacture at smaller scales than a two-phase design. The interior of the PUC (Fig. 1(a)) is considered to be void, and thus the wave propagation through this geometry is governed by the elastic wave equation:

$$\rho\ddot{\boldsymbol{u}} = (\lambda + 2\mu)\Delta\boldsymbol{u} - \mu\nabla\times\nabla\times\boldsymbol{u}, \tag{1}$$

where, $\boldsymbol{u}(\boldsymbol{r})$ and $\ddot{\boldsymbol{u}}(\boldsymbol{r})$ are the spatial displacement field and acceleration, respectively, and $\boldsymbol{r}$ is the position vector. ρ represents the density of the material, and λ and μ are the Lamé coefficients, whereas Δ and $\nabla\times$, respectively, are 2D Laplacian and curl operators. We consider polysulfone (PSU) to be the preferred material for the analysis with $\rho = 1350\,\text{kg/m}^3$, elastic modulus, $E = 5.18\,\text{GPa}$, and Poisson's ratio, $\nu = 0.37$.

We apply the Bloch–Floquet periodic boundary condition [15] while sweeping the wave vector through the IBZ (highlighted using solid lines in the Brillouin zone from Fig. 1(b), where $\boldsymbol{\Gamma} = \boldsymbol{0}$) to obtain the band structure response as shown in Fig. 1(c). The equation takes the following form:

$$\boldsymbol{u}_{n+1}(\boldsymbol{r}) = e^{\imath\boldsymbol{k}\cdot\boldsymbol{a}_i}\boldsymbol{u}_n(\boldsymbol{r}), \tag{2}$$

where n is the PUC's index, $\boldsymbol{k} = (\boldsymbol{k}_x, \boldsymbol{k}_y)$ is the wave vector in 2D [20], $\boldsymbol{a}_i = (\boldsymbol{a}_x, \boldsymbol{a}_y)$ is the lattice vector, where $\|\boldsymbol{a}_x\| = \|\boldsymbol{a}_y\| = a$, and $\imath$ is the complex number. The upper and lower wavebands bounding the BG are also marked in Fig. 1(c). Starting from the given PUC, we would like to design another PUC that possesses PBGs (BGs only in specific ranges of the wave vector) instead. In that case, we need to influence these bounding modes and create localized changes in the band structure. Since geometry changes to the PUC may break its symmetry, we may also need to change the IBZ and sweep through more branches to obtain a complete band structure [21]. We instead use a half Brillouin zone (HBZ) from the beginning, as any change in the geometry can be accommodated by the band structure without modifying the HBZ [21]. Fig. 2(b) shows the same PUC from Fig. 1(a), with an HBZ, and Fig. 2(a) shows the corresponding band structure represented using dotted curves. Fig. 2(c) also shows a few displacement modes (marked with arrows in Fig. 2(a)), which are selected at the HBZ's first three branches' midpoints. The band structure and displacement modes are obtained via the $\omega(\boldsymbol{k})$ approach using finite element analysis [22] by solving the wave equation (1) subjected to Bloch–Floquet periodic boundary condition (2). The superscripts L and U represent points on the lower and upper BG wavebands (bounding bands) within the band structure. To tune the band structure locally, we make necessary modifications to the geometry, changing the corresponding displacement mode by locally changing the stiffness or mass using concepts from basic mechanics. Noteworthy is that the modifications in the geometry are not particular to the initial design since the changes are based on displacement modes that can be applied to any selected initial design. Take, for instance, t_1 through t_4 and A_1 through A_4 as design parameters (refer Fig. 2(b)). These can be considered as springs and masses with the associated behaviors. Increasing thicknesses t_2 and t_4, in turn, increases stiffnesses (and, in effect, frequencies) of D_1^L and D_3^L more than D_2^L since the latter is a combination of axial and bending modes, which turns to a bending dominated mode because of the asymmetries introduced (see the transition of the 3rd waveband in Fig. 2(a)). Similarly, for masses, removing material from the center of rotation has minimal effect on rotating modes (*e.g.,* D_2^U) while having a substantial effect on translational modes (*e.g.,* D_1^U). The effect of local changes can then be visualized by regenerating the band structure, as we have done in Fig. 2(a).

3. Partial band gap generation by manipulating displacement modes

Our objective is to obtain the topology of the PUC for the desired band structure. As an example, we want to create a geometry with a band structure possessing PBGs, which allow the propagation of waves with short wavelengths closer to $\boldsymbol{k} = \boldsymbol{\Gamma}$ while attenuating the rest of the waves (refer Fig. 3(b)). This peculiar property would allow the PnC structure to act as a polarizer for shear (S) waves, *i.e.,* it permits the propagation of S waves while suppressing pressure (P) waves in the same direction. Consider, for instance, the initial PUC and the band structure (Fig. 2). We need to manipulate the bounding bands (3rd and 4th bands) such that they intersect at a particular position (in the current case at $\boldsymbol{k} = \boldsymbol{\Gamma}$). So we increased the thicknesses t_2 and t_4, which resulted in an increase in stiffness (as mentioned already); therefore, corresponding points (from 3rd band) in the band structure moved up. To further locally tune the band structure, we introduced additional asymmetries by supplying t_1 through t_4 with linearly variable thicknesses, thus moving only the points of the lower BG waveband near $\boldsymbol{k} = \boldsymbol{\Gamma}$ up. Further, A_1 and A_4 were increased (thus increasing the corresponding masses), which resulted in shifting down the 4th band closer to $\boldsymbol{\Gamma}$. We repeated this process for a few more steps and obtained PBGs in the band structure. Fig. 3(a) shows the initial and modified band structures, where we can see the shifting of the upper and lower BG wavebands till they intersect. Fig. 3(b) and (c) respectively represent the corresponding PUC geometry and displacement modes. All design steps, together with their corresponding PUCs, band structures, and selected displacement modes, are provided in the supplementary material. It should be noted that the redistribution of the material reduced the contrast in the stiffness and mass between the adjacent phases within the PUC, thus reducing the BG width. A transmission analysis is performed on an 8×8 PnC waveguide array to verify the band structure, whose geometry and the result are also provided in the supplementary material. Transmission of S waves shows more than two orders of magnitude compared to P waves traveling in the same direction; thus, we can infer that the obtained PnC design is an S wave polarizer.

4. Introducing resonator modes to create partial band gaps

Instead of making local changes to the PUC, a PBG could also be obtained by introducing a resonator. These resonators can produce BGs (due to local resonance), as in the case of an acoustic metamaterial [23,24]. By tuning the frequency and the spatial orientation of

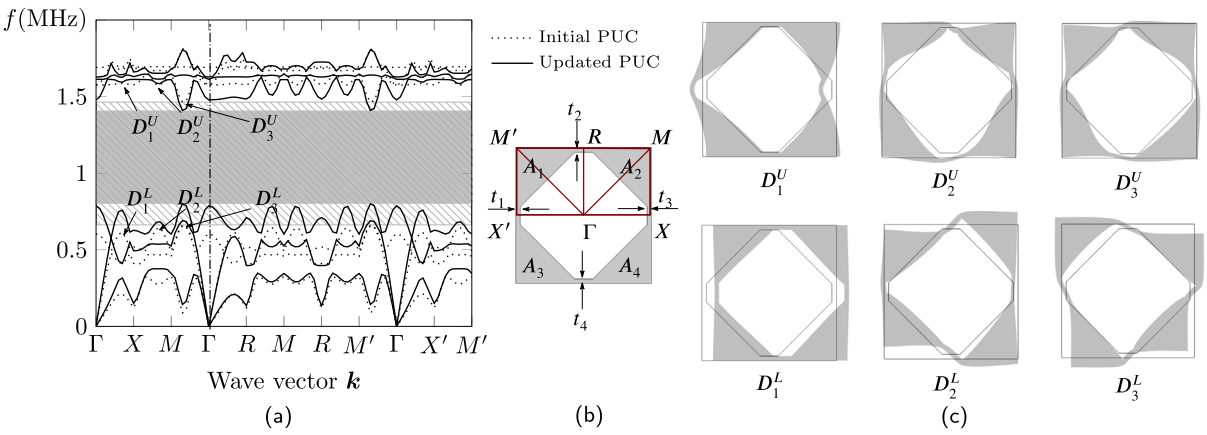

Fig. 2. Schematic showing (a) band structures of initial and updated PUCs with hatched and shaded regions showing corresponding BGs, (b) Initial PUC with HBZ, and (c) relevant displacement modes. The PUC has been segmented to different portions such as thicknesses of ribs (t_1 through t_4) and areas of triangular shapes (A_1 through A_4). D_1 through D_3 are three displacement modes from the first three branches of the HBZ corresponding to the BG. Superscripts L and U respectively represent lower and upper BG wavebands.

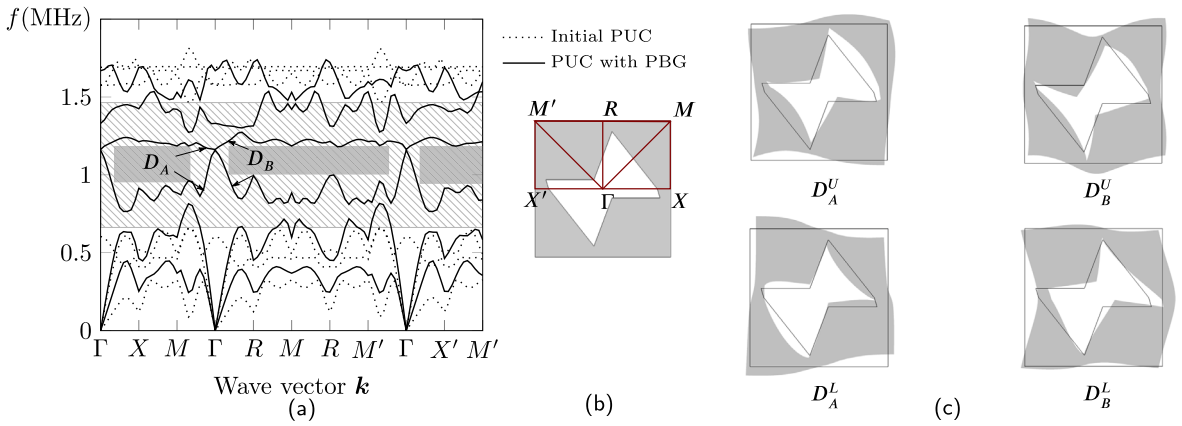

Fig. 3. Schematic representing (a) Band structures of the initial and modified PUCs where hatched and shaded regions respectively show the initial BG and updated PBGs, (b) modified PUC with HBZ, and (c) corresponding displacement modes. D_A and D_B are displacement modes close to the separation of two BGs by a transmission region. Their locations in the bandstructure are marked in (a).

the resonator, PBGs can be generated at a given frequency range in the original band structure (without the resonator). However, the introduction of the resonator changes the PUC topology, which may result in drastic changes in the existing band structure depending upon the level of coupling between the modes of the resonator and the remaining PUC. Adding a resonator at a 45° to the PUC from Fig. 2 results in a strong coupling between their modes because the resonator is connected to the stiffer portion of the PUC. Thus we cannot create a localized change in the band structure. Therefore no PBGs can be created (the geometry, band structure, and relevant displacement modes are available in the supplementary material). Hence, to obtain a PBG, we need to have a weak coupling between these modes (in the current case, modes from the lower BG waveband and the adjacent waveband introduced by the resonator), such that changes in the desired resonator mode have limited influences to the rest of the band structure.

For instance, by adding a resonator connected vertically to the PUC of Fig. 2(a) (see Fig. 4(b)), we could introduce additional bands within the BG of the initial PUC (as represented by solid curves in Fig. 4(a)). D_A^L and D_B^L From Fig. 4(c) are displacement modes corresponding to the points of the lower BG waveband of the PUC. Since this band and corresponding displacement modes are similar to the original PUC from Fig. 2 (although D_B^L shows 90° rotation to that of D_1^L because the corresponding wave vector experiences the same rotation), we can state that the resonator and the remaining PUC modes have a weak coupling. Because, in the vertical orientation, the resonator is connected to the flexible region of the PUC, thus, reducing their interactions. However, both D_A^U and D_B^U are almost exclusively resonator modes; hence, we can tune the corresponding band locally by changing these modes (D_A^U and D_B^U) with minimal effects on the rest of the band structure.

To create the PBG, we can bring this resonator-dominant waveband closer to the lower BG waveband by reducing its frequency. For instance, by increasing the area of the central square of the resonator, as shown in Fig. 5(b), we could increase its mass to bring down the frequency of the upper waveband. Fig. 5(a) shows the band structures of the PUC with the resonator and the PUC with an updated resonator where the upper and lower wavebands are connected at $\boldsymbol{k} = \boldsymbol{\Gamma}$ to form partial BGs. The corresponding displacement modes (see Fig. 5(c)) are virtually identical to that of the initial resonator (see Fig. 4(c)), implying that the changes in the resonator did not modify the modes. In comparison with the previous case (tuning existing bands to obtain the desired band structure behavior), a resonator allows placing additional wavebands at desired locations in the band structure. Moreover, the changes in the resonator have very localized effects on the band structure (they affect the resonator wavebands). This can also be verified by the fact that the lower waveband, where BG begins, experienced few changes due to the introduction and modification of the resonator (see Figs. 4(a) and 5(a)). Similar to the previous case described in Section 3, a transmissibility analysis can be performed on a finite PnC waveguide based on the PUC (Fig. 5(b)) geometry. Since the procedure is the same as described in the supplementary material, we avoid it for brevity.

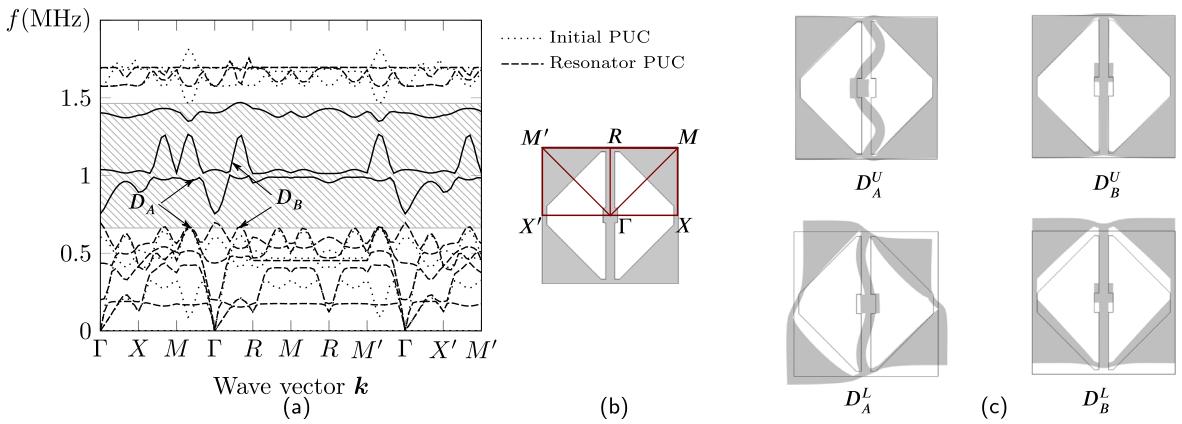

Fig. 4. (a) comparison of band structures between initial and resonator PUCs where the resonator introduced wavebands are shown using solid curves, while the hatched region represents the former's BG, (b) schematic of the PUC with a vertical resonator and its HBZ, and (c) relevant displacement modes.

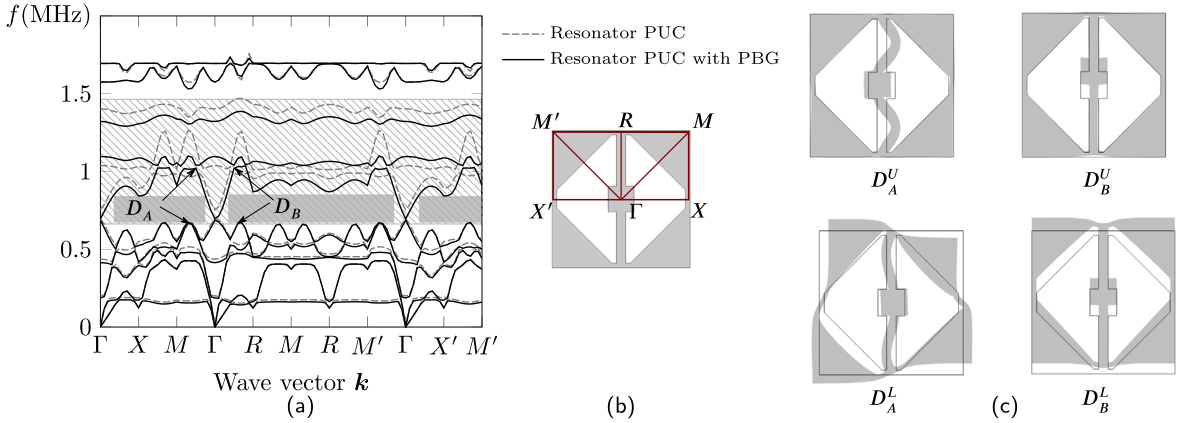

Fig. 5. (a) Band structure comparison between PUC with a resonator and the PUC with the modified resonator, where hatched and shaded regions are the BG of the initial PUC, and PBGs of the PUC with modified resonator, (b) schematic of the resonator PUC with HBZ, and (c) relevant displacement modes.

5. Conclusion

In this work, we proposed an approach to understand the link between PUC geometry and the band structure effectively, and we showed that it can be used to make predictable changes to the band structure by locally tuning the PUC by either changing the geometry or by introducing a resonator. These local modifications follow from straightforward mechanics' principles. Starting from a given PUC geometry and its corresponding band structure, we showed that PBGs could be generated by following this approach, resulting in a new geometry by tuning the relevant displacement modes. We also demonstrated that we can manipulate the band structure further by introducing resonators with particular resonance frequencies and spatial orientations. By tuning distinct resonator modes after studying their influence on the band structure, we effectively generated PBGs. Thus, we conclude that this displacement mode-based approach is a useful tool for BG manipulation and tuning the band structure for PnCs and PnC-inspired components. Moreover, we could use the results of this approach as initial designs for further tuning by systematic computational tools such as topology optimization.

CRediT authorship contribution statement

Sabiju Valiya Valappil: Conceptualization, Methodology, Software, Writing – original draft. **Alejandro M. Aragón:** Writing – review & editing, Supervision. **Hans Goosen:** Conceptualization, Methodology, Writing – review & editing, Supervision.

Declaration of competing interest

The authors declare that they have no known competing financial interests or personal relationships that could have appeared to influence the work reported in this paper.

Data availability

Data will be made available on request.

Acknowledgments

We gratefully appreciate the support from Topconsortia voor Kennis en Innovatie (TKI) project grant and our sponsoring partner Krohne.

Appendix A. Supplementary data

Supplementary material related to this article can be found online at https://doi.org/10.1016/j.ssc.2022.115061.

References

[1] M.S. Kushwaha, P. Halevi, L. Dobrzynski, B. Djafari-Rouhani, Acoustic band structure of periodic elastic composites, Phys. Rev. Lett. 71 (1993) 2022–2025.
[2] M.S. Kushwaha, P. Halevi, G. Martínez, L. Dobrzynski, B. Djafari-Rouhani, Theory of acoustic band structure of periodic elastic composites, Phys. Rev. B 49 (1994) 2313–2322.
[3] W.L. Bragg, The diffraction of short electromagnetic waves by a crystal, Scientia 23 (45) (1929) 153.

[4] Matthew Reynolds, Stephen Daley, An active viscoelastic metamaterial for isolation applications, Smart Mater. Struct. 23 (4) (2014) 045030.
[5] Kyung Ho Sun, Jae Eun Kim, Jedo Kim, Kyungjun Song, Sound energy harvesting using a doubly coiled-up acoustic metamaterial cavity, Smart Mater. Struct. 26 (7) (2017) 075011.
[6] Shu Zhang, Leilei Yin, Nicholas Fang, Focusing ultrasound with an acoustic metamaterial network, Phys. Rev. Lett. 102 (19) (2009) 194301.
[7] J. Xu, J. Tang, Tunable prism based on piezoelectric metamaterial for acoustic beam steering, Appl. Phys. Lett. 110 (18) (2017) 181902.
[8] Zhaojian He, Feiyan Cai, Zhengyou Liu, Guiding acoustic waves with graded phononic crystals, Solid State Commun. 148 (1) (2008) 74–77.
[9] Shu Zhang, Chunguang Xia, Nicholas Fang, Broadband acoustic cloak for ultrasound waves, Phys. Rev. Lett. 106 (2) (2011) 024301.
[10] Mahdiyeh Ghoreshi, Ali Bahrami, Acoustic invisibility cloak based on two-dimensional solid-fluid phononic crystals, Solid State Commun. 342 (2022) 114646.
[11] A.A. Maznev, A.G. Every, O.B. Wright, Reciprocity in reflection and transmission: What is a 'phonon diode'? Wave Motion 50 (4) (2013) 776–784.
[12] Osama R. Bilal, André Foehr, Chiara Daraio, Bistable metamaterial for switching and cascading elastic vibrations, Proc. Natl. Acad. Sci. 114 (18) (2017) 4603–4606.
[13] Karl F. Graff, Wave Motion in Elastic Solids, Courier Corporation, 2012.
[14] Hendrik J. Monkhorst, James D. Pack, Special points for Brillouin-zone integrations, Phys. Rev. B 13 (1976) 5188–5192.
[15] Felix Bloch, Quantum mechanics of electrons in crystal lattices, Z. Phys. 52 (1928) 555–600.
[16] Ze-Guo Chen, Ying Wu, Tunable topological phononic crystals, Phys. Rev. Appl. 5 (2016) 054021.
[17] Bo Yuan, Bin Liang, Jian-cheng Tao, Xin-ye Zou, Jian-chun Cheng, Broadband directional acoustic waveguide with high efficiency, Appl. Phys. Lett. 101 (4) (2012) 043503.
[18] Xiasheng Guo, Zhou Lin, Juan Tu, Bin Liang, Jianchun Cheng, Dong Zhang, Modeling and optimization of an acoustic diode based on micro-bubble nonlinearity, J. Acoust. Soc. Am. 133 (2) (2013) 1119–1125.
[19] Jingjie He, Zhan Kang, Achieving directional propagation of elastic waves via topology optimization, Ultrasonics 82 (2018) 1–10.
[20] A. Bedford, D.S. Drumheller, Elastic Wave Propagation, John Wileg G Sons, 1994, pp. 151–165.
[21] Florian Maurin, Claus Claeys, Elke Deckers, Wim Desmet, Probability that a band-gap extremum is located on the irreducible brillouin-zone contour for the 17 different plane crystallographic lattices, Int. J. Solids Struct. 135 (2018) 26–36.
[22] L. D'Alessandro, E. Belloni, R. Ardito, A. Corigliano, F. Braghin, Modeling and experimental verification of an ultra-wide bandgap in 3D phononic crystal, Appl. Phys. Lett. 109 (22) (2016) 221907.
[23] Steven A. Cummer, Johan Christensen, Andrea Alù, Controlling sound with acoustic metamaterials, Nat. Rev. Mater. 1 (3) (2016) 16001.
[24] Guancong Ma, Ping Sheng, Acoustic metamaterials: From local resonances to broad horizons, Sci. Adv. 2 (2) (2016) e1501595.